American Mineralogist, Volume 90, pages 779–789, 2005

Factors in the preservation of coesite: The importance of fluid infiltration

JED L. MOSENFELDER,[1,*] HANS-PETER SCHERTL,[2] JOSEPH R. SMYTH,[3] AND JUHN G. LIOU[4]

[1]Division of Geological and Planetary Sciences, California Institute of Technology, M/C 170-25, Pasadena, California 91125, U.S.A.
[2]Institut für Geologie, Mineralogie und Geophysik, Ruhr-Universität Bochum, D-44780 Bochum, Germany
[3]Department of Geological Sciences, University of Colorado, Boulder, Colorado 80309-0399, U.S.A.
[4]Department of Geological and Environmental Sciences, Stanford University, Stanford, California 94305-2115, U.S.A.

ABSTRACT

The survival of coesite in ultrahigh-pressure (UHP) rocks is most commonly attributed to rapid exhumation, continuous cooling during uplift, and inclusion in strong phases that can sustain a high internal over-pressure during decompression. Exceptions to all of these criteria exist. Perhaps less attention has been paid to the role of fluid infiltration in the preservation of coesite. We used infrared spectroscopy to measure water contents of coesite and coesite pseudomorphs in a variety of UHP rocks. In all cases, OH concentrations in coesite are below the detection limit of ~100 ppm H_2O. The silica phases surrounding coesite, however, show varying amounts of H_2O. This is most spectacularly observed in pyrope quartzites from the Dora-Maira massif that contain at least three phases of silica replacing coesite, also distinguished by varying color of cathodoluminescence (CL): palisade-textured quartz (<100 ppm H_2O, red-violet CL); "mosaic" quartz, which is actually chalcedony (up to 0.4 wt% H_2O, yellow/brown CL); and a rare, highly hydrated silica phase interpreted to be opal (~7 wt% H_2O, dark blue CL). Very similar signatures are observed in a grospydite xenolith from the Roberts Victor kimberlite. The quartz replacing coesite in other UHP samples studied contains on the order of 500 ppm H_2O or less, and most measurements are under the detection limit of our technique. We infer that palisade quartz forms under dry or nearly dry conditions and at high temperatures during dilation of the host phase. The formation of hydrous silica phases such as chalcedony and opal, however, must take place at much lower temperatures, after cracking of the host phase, which allows external fluids to infiltrate. Delay of fluid infiltration to low temperatures, where kinetics are slow even in the presence of water, is the most critical factor in the preservation of coesite.

INTRODUCTION

Although coesite inclusions in eclogitic diamond were first reported by Sobolev et al. (1976), coesite and quartz pseudomorphs after coesite were first identified and fully described in an eclogitic rock by Smyth and Hatton (1977; see also Smyth 1977). The discovery of coesite in regionally metamorphosed rocks of the Dora-Maira massif (Western Alps) by Chopin (1984) proved for the first time that continental crust has been subducted to depths of 100 km or more and subsequently returned to the surface of the Earth. This remarkable finding galvanized the field of metamorphic petrology and spurred multi-disciplinary progress in our understanding of the tectonics of continental collision and mountain building. One enduring question for petrologists is how to explain the preservation of coesite, which is highly metastable at low pressures and should revert easily to quartz during exhumation of the host rocks from such great depths. Four major factors required for the survival of coesite were invoked by Chopin (1984), and they remain the most commonly cited criteria in more recent literature (e.g., Hacker and Peacock 1995; Ernst 1999, 2001). Perhaps the most critical factor is thought to be its inclusion in strong host phases, such as garnet and zircon, which can act as "pressure vessels" and sustain an overpressure on the inclusion, inhibiting the volume increase necessary to transform to quartz (Gillet et al. 1984; van der Molen and van Roermund 1986). Other factors considered to be important are rapid exhumation, continuous cooling during decompression, and prevention of fluid infiltration into the host mineral until fracturing at low temperatures.

In the last two decades following the initial discovery, coesite has been found in numerous other localities and some challenges to the above hypotheses have appeared. Discovery of coesite (and/or its well-preserved pseudomorphs) as inclusions in the volatile-bearing and relatively weak phases dolomite (Schertl and Okay 1994; Zhang and Liou 1996), tourmaline (Reinecke 1991), zoisite (Zhang et al. 1995a), epidote (Enami et al. 2004), apatite (Reinecke 1998), and wagnerite (Brunet et al. 1998) poses difficulties for the "pressure vessel hypothesis," as does the extremely rare finding of intergranular coesite, sandwiched between two or more minerals (Liou and Zhang 1996; Wallis et al. 1997).

Rapid exhumation in most UHP terranes has now been confirmed with geochronological data (Gebauer et al. 1997; Amato et al. 1999; Rubattto and Hermann 2001; Carswell et al. 2003; Hacker et al. 2003; Treloar et al. 2003). However, uncertainties remain as to the residence time of some UHP rocks at elevated temperature within the middle or upper crust (e.g. Walsh and Hacker 2004), following an initial period of rapid exhumation

* E-mail: jed@gps.caltech.edu

from UHP depths. This issue is important because experimental kinetic studies (Mosenfelder and Bohlen 1997; Perrillat et al. 2003) suggest that even short residence times (on the order of 1 m.y.) at modest temperatures (ca., 400 °C) may be enough to transform coesite completely. The criterion of continuous cooling during exhumation has also failed in some cases where granulite-facies overprints have been recognized (Wang et al. 1993; Nakamura and Hirajima 2000), or nearly isothermal decompression at high temperature has been inferred (Lardeaux et al. 2001; Ghiribelli et al. 2002).

Increasing attention has been paid in recent years to the influence of limited fluid availability in inhibiting the kinetics of both prograde and retrograde metamorphism. Evidence for heterogeneous and highly restricted fluid flow in UHP rocks comes from both petrographic and fluid inclusion studies (e.g., Philippot et al. 1995; Liou and Zhang 1996; Zhang and Liou 1997; Fu et al. 2001) and stable isotope studies (see Zheng et al. 2003 for review). However, only a few studies have produced data bearing directly on the role of fluids in the coesite to quartz transformation (e.g., Philippot et al. 1995; Langenhorst and Poirier 2002). In the present study, we addressed this issue using Fourier-Transform infrared spectroscopy (FTIR) to measure the water contents of coesite and associated phases in UHP-metamorphic rocks. Cathodoluminescence (CL) microscopy was also used to investigate textures of coesite and its pseudomorphs in two samples. The investigated samples included pyrope-quartzite from the Dora-Maira massif, eclogites from the Dabie Shan and Sulu terranes (eastern China), and eclogites from the Western Gneiss Region of Norway. Sample 95YK4E from the Sulu region is of particular interest because it contains grains of intergranular coesite (Liou and Zhang 1996). We also analyzed intergranular coesite and coesite pseudomorphs in a mantle xenolith (SRV-1) from the Roberts Victor Mine kimberlite, South Africa (Smyth 1977).

Using the CL technique, Schertl et al. (2004) identified the presence of hydrous silica (chalcedony) replacing coesite in rocks from the Dora-Maira massif; herein we report for the first time the surprising replacement of coesite by an orbicular-textured phase interpreted to be opal (Fig. 1).

Analytical methods

Coesite is usually easy to recognize optically because of its high refractive index. Where necessary, we used Raman spectroscopy to verify the identity of coesite by the presence of its characteristic peak at 521 cm^{-1} (Boyer et al. 1985). Raman patterns were collected using a Renishaw Micro Raman spectrometer operating with a 514.5 nm Ar ion laser.

The techniques used for cathodoluminescence microscopy have been described by Schertl et al. (2004). For infrared work, doubly polished sections with thicknesses of ~50–80 µm were prepared using Crystalbond adhesive, which was later dissolved in acetone. After removal of Crystalbond, the sections were cleaned in ethanol. Section thicknesses were measured using a digital micrometer and verified using an optical microscope (Libowitzky and Rossman 1997) and are considered accurate to ±3 µm.

Infrared spectra were acquired using a Nicolet Magna 860 FTIR spectrometer coupled to a Spectra-Tech Continuum microscope with a continuously adjustable motorized aperture system. Nominally unpolarized spectra in the mid-IR and near-IR regions were recorded by averaging 400 scans with 2 cm^{-1} resolution, using an infrared light source, CaF_2 or KBr beamsplitter, and MCT-A detector. Most analyses were made using 20–100 µm diameter square apertures; in the case of one inclusion, we collected spectra using a 10 × 50 µm rectangular aperture. In favorable cases, this procedure allowed selection of areas free of cracks and other phases, but for particularly small, well-preserved coesite inclusions, overlap between phases and/or measurement through cracks was unavoidable.

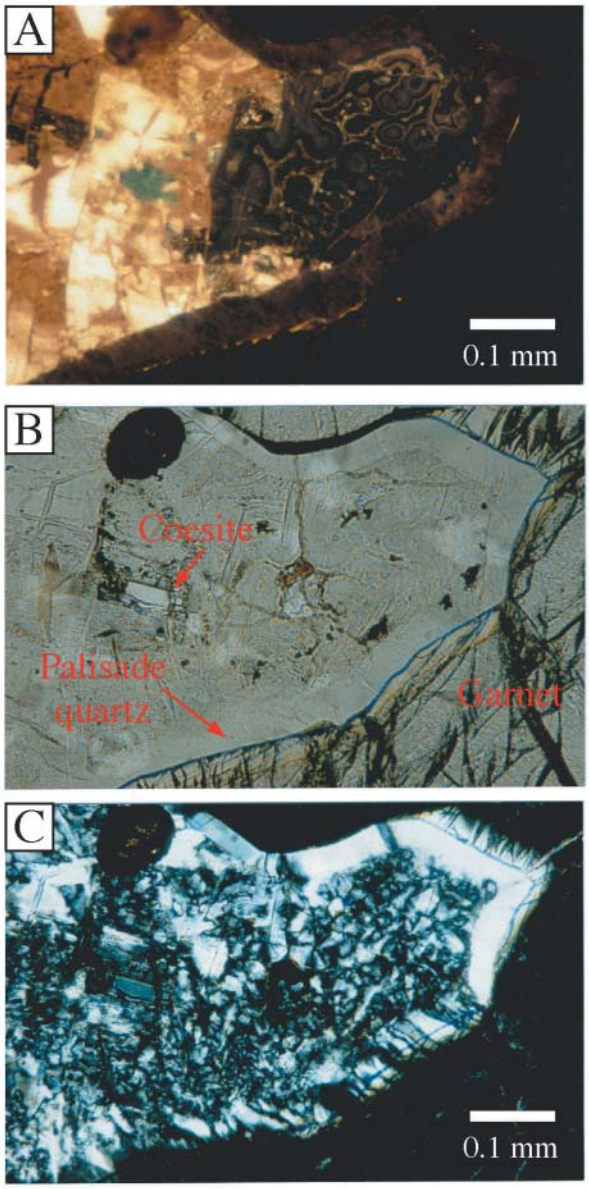

Figure 1. An unusual inclusion in garnet in Dora-Maira fine-grained pyrope quartzite. (**a**) CL image showing agate-like, orbicular microstructures in silica replacing coesite. Chalcedony, palisade quartz, and coesite display yellowish-brown, red, and blue CL, respectively. (**b**) Plane-polarized light. (**c**) Cross-polarized light.

Calculation of H_2O and OH concentrations

Water contents of natural quartz in the literature have been estimated using at least three different calibrations. Nakashima et al. (1995) used the Beer-Lambert law:

$$A = \varepsilon \times c \times d$$

where A is the maximum band height (absorbance) at 3400 cm^{-1}, ε is the molar absorption coefficient of liquid water (0.81 L/mol cm), c is concentration (in mol/L), and d is thickness (in cm)

of the sample. In an earlier study, Kronenberg and Wolf (1990) used a modified form of the Beer-Lambert law:

$$A_i = I \times c \times d$$

where A_i is the integral absorption of the band area over the 3400 cm^{-1} region, I is the integral molar absorption coefficient (in L/mol·cm^2), and c is concentration expressed as H/10^6 Si. They used a value for I of 0.812 (cm^2 H/10^6 Si), which was determined for sharp bands in natural quartz. For comparison with these previous studies, we report calculated values using both calibrations (Table 1), with all concentrations converted to ppm H_2O by weight. Each of these approaches has its limitations. Measurements of peak heights are inherently less accurate than measurements of integral absorption (e.g., Libowitzky and Rossman 1997), but the calibration used by Kronenberg and Wolf (1990) has the disadvantage of being based on sharp band (OH defect) absorption rather than the broadband (liquid H_2O) absorption commonly seen in larger amounts in natural quartz. Aines et al. (1984) determined a higher calibration factor of 1.05 (cm^2 H/10^6 Si) for broadband absorption in synthetic quartz. We also report calculated values using this factor in Table 1. Note that some spectra (see below) show evidence for narrow bands, representing OH defects, in addition to the broadband absorption related to liquid H_2O. Although these narrow bands are polarized, the use of unpolarized radiation in this study is justified due to the very fine grain size of the material. We made no attempt to differentiate the concentrations associated with OH defects, which are a small contribution to the overall H_2O content.

In the case of opal, we measured integral absorption (A_i) in the NIR region to calculate H_2O and OH concentrations, using integral molar absorption coefficients of 250 L/mol·cm^2 for H_2O (5200 cm^{-1} band) and 160 L/mol cm^2 for OH (4500 cm^{-1} band) (Langer and Flörke 1974) (Table 2). Assumptions about density for this phase are discussed below.

Detection limits were an important issue in estimating the water content of quartz replacing coesite in small inclusions. Detection limits for a given mineral depend primarily on sample thickness, aperture width, wavenumber resolution, and number of scans. We estimated the limit to be three times the signal to noise ratio for each condition (Thomsen et al. 2003). For example, for a 100 × 100 µm aperture, 50 µm thick sample and 400 scans, the limit is estimated to be 100 ppm for H_2O in quartz; reducing the aperture size to 20 × 20 µm increases the limit to about 300 ppm. Running more scans with apertures as small as 20 × 20 µm did not appreciably improve the detection limit. Estimated detection limits for the representative spectra are given in Table 1.

FLUID SIGNATURES OF SILICA IN UHP ROCKS

Dora-Maira massif

We investigated sample 19485, a fine-grained pyrope quartzite (containing pyrope + talc + kyanite + phengite + quartz + jadeite) from the Parigi outcrop in the Dora-Maira massif, western Alps. The detailed petrology of rocks from the Parigi outcrop has been described by Schertl et al. (1991). Peak *P-T* conditions were estimated to be 3.7 GPa and 900 °C (Schertl et al. 1991). The textures of coesite/quartz inclusions in the Dora-

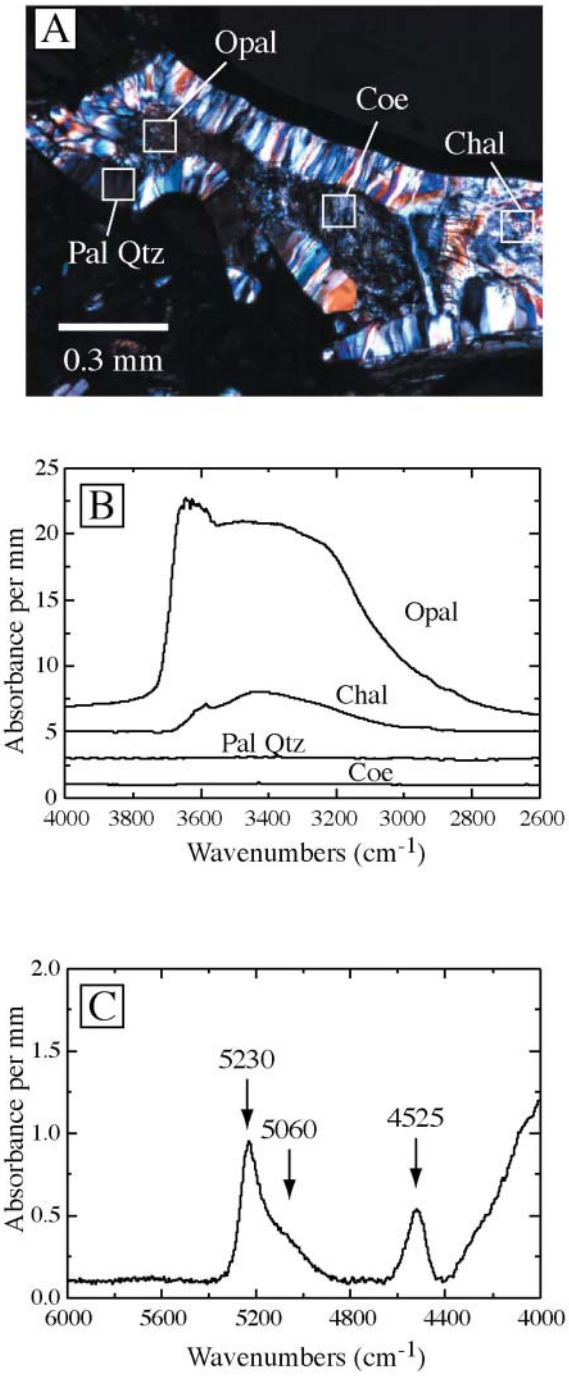

FIGURE 2. Infrared spectra of coesite (coe), opal, mosaic quartz (mos qtz), and palisade quartz (pal qtz) in an inclusion in garnet from Dora-Maira sample 19485. Spectra are normalized to 1 mm sample thickness and shifted vertically for clarity. (**a**) Photograph in cross-polarized light showing locations of analyses in b. (**b**) Mid-IR spectra. Note peak at 3585 cm^{-1} with a shoulder at 3615 cm^{-1} in mosaic quartz, typical of chalcedony. The structure of the peak around 3600 cm^{-1} in opal is not meaningful because the sample completely absorbed in this region. (**c**) Near-IR spectrum of opal showing combination bands (stretching and bending) of molecular H_2O (5230 cm^{-1}, with a shoulder at ~5060 cm^{-1}), and Si-OH groups (4525 cm^{-1}).

TABLE 1. Representative H_2O concentrations for silica phases in UHP rocks

Phase	aperture (μm)	d (cm)	Peak Height	Peak Area	Detection limit (ppm H_2O)	C (H_2O), ppm by weight		
						Method 1 Peak ht	Method 2 int abs	Method 3
Dora Maira pyrope-quartzite (19585)					0.812	1.05		
coe	100 × 100	0.008	0.004	2.500	60	n.d.	n.d.	n.d.
pal qtz	100 × 100	0.008	0.005	3.000	60	n.d.	n.d.	n.d.
mos qtz	100 ×100	0.008	0.163	78.912	60	1709	1201	1554
mos qtz	100 × 100	0.008	0.296	142.270	60	3103	2166	2801
mos qtz	100 × 100	0.008	0.365	178.968	60	3826	2725	3523
Dabie-Shan (Shuanghe) eclogite (94-62B)								
mat qtz	25 × 25	0.0054	0.005	5.508	250	n.d.	n.d.	n.d.
	Inclusion 1							
coe	10 × 50	0.0054	0.011	8.019	260	n.d.	n.d.	n.d.
pal qtz	10 × 50	0.0054	0.006	0.719	260	n.d.	n.d.	n.d.
	Inclusion 2							
coe	25 × 25	0.0054	0.012	10.742	250	n.d.	n.d.	n.d.
pal qtz	25 × 25	0.0054	0.029	17.974	250	450	405	524
	Inclusion 3							
mos qtz	25 × 25	0.0054	0.021	13.980	250	320	315	408
Sulu (Yangkou Beach) eclogite (95YK-4E)								
	intergranular coesite							
mos qtz	25 × 25	0.0056	0.021	15.508	240	314	328	424
coe/qtz	25 × 25	0.0056	0.020	13.630	240	299	296	383
	intergranular pseudomorph							
mos qtz	25 × 25	0.0047	0.025	10.940	285	446	284	367
Norwegian (Otnheim) eclogite (aw370)								
coe/qtz*	25 × 25	0.006	0.010	3.531	225	n.d.	n.d.	n.d.
mat qtz	25 × 25	0.006	0.020	6.442	225	277	131	169
Roberts Victor Mine xenolith (SRV-1)								
coe	50 × 50	0.0058	0.003	3.248	160	n.d.	n.d.	n.d.
pal qtz	20 × 20	0.0058	0.034	15.474	160	492	325	420
mos qtz	50 × 50	0.0058	0.108	50.060	160	1561	1051	1359
mos qtz	50 × 50	0.0058	0.165	84.933	160	2386	1784	2306
mos qtz	50 × 50	0.0058	0.203	96.157	160	2935	2019	2611

Notes: coe = coesite; pal qtz = palisade quartz; mos qtz = mosaic quartz; mat qtz = matrix quartz; coe/qtz = mixed phase coesite + quartz.
* Inclusion composed of ~90% coesite, 10% quartz.

Maira pyrope quartzites are well known and have been used as diagnostic features to identify pseudomorphs after coesite in many other localities. Relict coesite is invariably surrounded by a polycrystalline rim of fine-grained, elongated quartz crystals with a radiating texture (Chopin 1984). This "palisade quartz" sometimes coexists with even finer-grained quartz, referred to as diffuse quartz (Gillet et al. 1984) or mosaic quartz (e.g., Mosenfelder and Bohlen 1997). The formation of this latter type of quartz has been associated with the development of cracks in the host phase and subsequent infiltration of fluids (Gillet et al. 1984). Schertl et al. (2004) investigated these inclusions using CL petrography and showed that the different phases of SiO_2 can be distinguished easily by their different CL colors: green-blue for coesite, violet-red for palisade quartz, and bright brownish-yellow for the mosaic quartz, which was inferred to be chalcedony. Figure 1 shows a previously unpublished CL micrograph of a Dora-Maira SiO_2-inclusion that shows these features, as well as a distinct orbicular "agate-like" texture, which suggests the presence of a water-rich silica phase. Although the origin of CL in these silica phases may depend on several factors, the differentiation between coesite and quartz appears to be robust in different UHP rocks (Schertl et al. 2004). The variation between quartz and chalcedony may be caused by variable water (or OH) content or perhaps some other trace-element distribution.

Our investigation using FTIR revealed systematic patterns of absorbance in the OH-stretching region for all of the different phases of SiO_2. Figure 2a shows a representative inclusion, with the locations of IR analyses presented in Figure 2b. Analyses of palisade quartz and uncracked crystals of coesite reveal no traces of H_2O or OH within the detection limit, in this case about 60 ppm. Transmission electron microscopy (TEM) revealed nanometer-sized fluid inclusions in both of these phases (Langenhorst and Poirier 2002). Microscopic fluid inclusions in palisade quartz have also been studied by Philippot et al. (1995), who noted that they were not present in all crystals. Our inability to detect H_2O in this phase is presumably a reflection of our higher detection limit than these other techniques, although there could be differences between the samples studied.

The spectra of the "diffuse" quartz are considerably more interesting, revealing an intense broadband absorption as well as a sharp peak at 3585 cm^{-1} with a shoulder at ~3615 cm^{-1}. The sharp peak at 3585 cm^{-1} is typical for chalcedony and other low-temperature, hydrothermal silica phases such as amethyst, moganite, quartzine, and synthetic hydrothermally grown quartz (Graetsch et al. 1985). This peak has been attributed to Si-OH located at structural defects. This band is not found in the spectra of higher-temperature metamorphic or igneous quartz (Kronenberg and Wolf 1990; Nakashima et al. 1995). Calculated concentrations of H_2O (Table 1) range from about 1700 to 3800 ppm and show no systematic correlation with location in the thin section or grain size. These contents are significantly higher than those measured previously in quartz (Kronenberg and Wolf 1990; Nakashima et al. 1995). Thus, the measured spectra are consistent with the attribution by Schertl et al. (2004) of this phase as chalcedony rather than quartz, although the water concentrations are on the low end of typical amounts for chalcedony (Graetsch 1994). Further circumstantial evidence supporting this identification lies in the observation that quartz replacing coesite has a high density of

brazil twins (Ingrin and Gillet 1986; Langenhorst and Poirier 2002), which are also characteristic of chalcedony (Graetsch 1994). Xu et al. (1998) suggested that these defects result from non-equilibrium crystallization and high nucleation rates, commensurate with growth from coesite at low pressures and temperatures.

The inclusion shown in Figure 2a also contains a small region of ultra-fine-grained material. Spectra taken of this material show complete absorbance in the mid-IR (from about 3650 to 3200 cm^{-1}), which was quite surprising given how thin the section was. Thus, no meaningful quantitative information can be gained from integrating the peak absorbance in this region. The near-IR, however, shows well-resolved bands that are combination modes of O-H and indicate the presence of both H_2O (band at 5230 cm^{-1}, with a shoulder at ~5060 cm^{-1}), and Si-OH defects (band at 4525 cm^{-1}). This spectrum is typical of either opal (Langer and Flörke 1974; Graetsch 1994) or chalcedony (Graetsch 1994). Attempts to classify this phase further with Raman spectroscopy (Ostrooumov et al. 1999) failed due to fluorescence of the sample. One difficulty in precisely determining the concentration of hydroxyl species in this material lies in the large uncertainty in its density; typical values for opal range from 2.0 to 2.2 g/cm^3 (Langer and Flörke 1974), whereas the density of chalcedony ranges from 2.5 to 2.65 g/cm^3 (Graetsch 1994). Even considering this uncertainty, however, the calculated total H_2O content (Table 2) of the phase varies from 5.76 to 7.13 wt%, far more than previously measured amounts for chalcedony (Graetsch 1994). We therefore tentatively identify this phase as microcrystalline opal, although a mixture of various phases (including moganite, for instance) is certainly possible.

Dabie-Sulu eclogites

We studied two samples from the Dabie-Sulu orogen, the largest tract of UHP rocks in the world. Sample 94-62B is a silica-rich, medium-grained eclogite from Shuanghe, Dabieshan, described by Liou et al. (1997). It contains a primary assemblage of garnet + omphacite + quartz/coesite + rutile, with partial replacement of omphacite by a symplectite of plagioclase + amphibole; peak metamorphic conditions are estimated to be 650–680 °C at $P > 2.7$ GPa (Liou et al. 1997). Sample 95YK-4E is from Yangkou near Qingdao in the Sulu region (Liou and Zhang 1996). This fine-grained eclogite (garnet + omphacite + kyanite + phengite + rutile + coesite/quartz) contains intergranular coesite as well as coesite inclusions in garnet and omphacite and lacks major evidence of retrograde metamorphism. Peak *P-T* is estimated at 790 °C at $P > 2.8$ GPa (Liou and Zhang 1996). This locality is also notable for the preservation of igneous textures in metamorphosed granite (Wallis et al. 1997) and gabbro (Zhang and Liou 1997).

Sample 94-62B has abundant inclusions of coesite (Fig. 3a) and quartz pseudomorphs after coesite (up to ~100 μm) in both garnet and omphacite. Omphacite is partially replaced by plagioclase + amphibole symplectites. Quartz in the matrix exhibits an unusual "mosaic" texture that has been interpreted as being related to the transformation from coesite (Mosenfelder and Bohlen 1997) due to its similarity with textures in coesite pseudomorphs as well as experimentally produced textures. FTIR measurements failed to reveal the presence of H_2O in this quartz (Table 1). We also measured IR spectra on 12 inclusions of coesite and pseudomorphs after coesite in this sample; a representative example is shown in Figure 3 and data for three inclusions are given in Table 1. As in the Dora-Maira samples, analyses of uncracked coesite reveal no traces of H_2O or OH. Analyses of quartz range from being under the detection limit to up to 450 ppm H_2O.

In the section of sample 95YK-4E prepared for IR analysis, we located one grain of partially transformed intergranular coesite (Fig. 4a) and one completely transformed pseudomorph after coesite. Surprisingly, measured concentrations of H_2O in the intergranular pseudomorphs after coesite appear to be significant (Table 1). Note that we were not able to locate examples of better-preserved coesite such as the one shown in Figure 2 in Liou and Zhang (1996).

Norwegian eclogites

Coesite was discovered in the Western Gneiss Region (WGR) of Norway (Smith 1984) shortly after the discovery in the Dora-Maira massif. A widespread UHP province has been defined based on more recent discoveries (Wain 1997; Cuthbert et al. 2000; Wain et al. 2000). With difficulty, due its rare occurrence in these rocks compared with other UHP terranes, we located coesite and coesite pseudomorphs included in omphacite in two eclogites from the Stadlandet UHP province: aw370 from Otnheim and aw643 from Liberholmen. Detailed petrography and locations of these rocks are reported by Wain et al. (2000), and the peak *P-T* conditions were estimated to be >2.79 GPa and >790 °C, respectively (Wain 1997). Both samples contain retrograde amphibole, and Wain et al. (2000) reported an example where radial cracks in garnet extending outward from a coesite inclusion cut an amphibole vein, indicating that fracturing of the garnet occurred after amphibolite-facies retrogression.

Measurements on these inclusions were difficult to make due to their small size (~30–40 μm in diameter), and the amount of preservation of the inclusions was such that rims of quartz surrounding coesite were very thin (10 μm or less). Even with the use of small apertures, overlap between phases was unavoidable. Thus, although no H_2O was detectable in either quartz or coesite (Table 1), our method may not be sensitive enough to detect H_2O that could be present in thin rims of quartz.

Roberts Victor kimberlite

Sample SRV-1 is a well-studied grospydite xenolith from the Roberts Victor kimberlite (e.g., Smyth 1977, 1980; Smyth and Hatton 1977; Wohletz and Smyth 1984; Sharp 1992). The original sample was a rounded eclogite inclusion approximately 20 × 20 × 10 cm in size in a diamondiferous kimberlite. The characteristic textures of quartz pseudomorphs after coesite were first reported from this rock (Smyth 1977); these textures are essentially identical to those of silica inclusions in Dora-Maira pyrope quartzites and many other UHP rocks. Partially transformed coesite grains up to 3 mm in dimension coexist in (former) equilibrium with omphacite, garnet, kyanite, and sanidine. The sample also contains diamond up to 300 μm in diameter, and equilibration conditions are estimated to be 4.9 GPa and 1060 °C (Wohletz and Smyth 1984). All of these phases, with the exception of kyanite, are altered to various extents. The omphacite is highly altered as a result of exsolution of Ca-Tschermaks component and quartz (Smyth 1980).

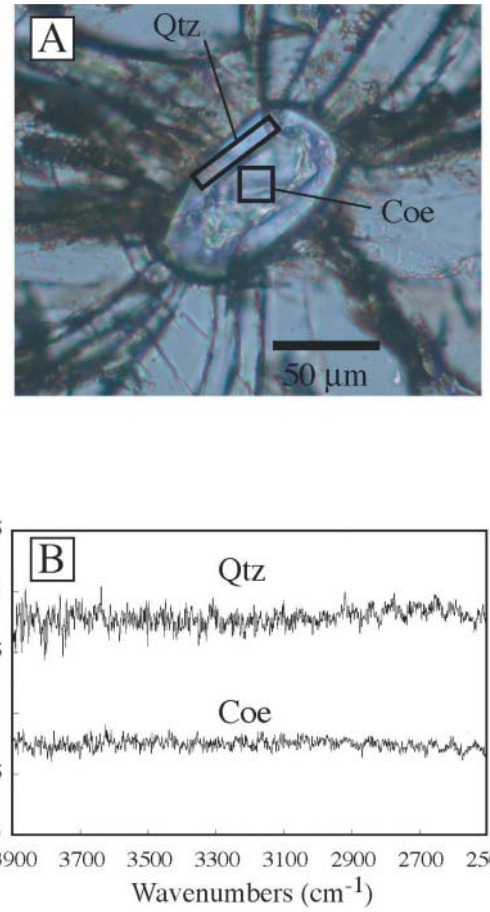

FIGURE 3. (**a**) Inclusion of coesite (coe) with a rim of quartz (qtz) included in garnet in sample 94-62B (Shuanghe, Dabieshan). Rectangular and square boxes show locations of analyses in **b**. Plane-polarized light. Scale bar = 50 µm. (**b**) Mid-IR spectra of coesite and quartz, showing lack of absorbance above detection limit. Spectra normalized to 1 mm thickness and shifted vertically for clarity.

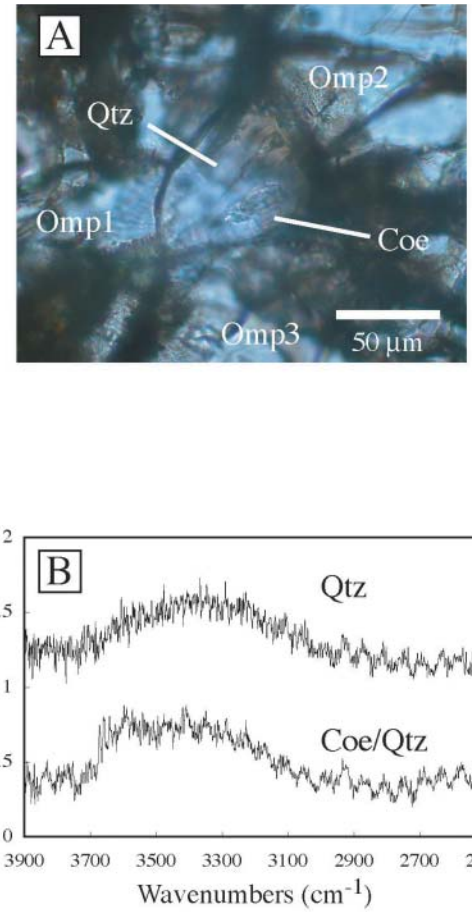

FIGURE 4. (**a**) An intergranular coesite (coe) crystal, mostly transformed to quartz (qtz), in sample 95YK-4E (Yangkou Beach, Sulu). Strings of relict coesite are preserved; the coesite has a higher refractive index than the surrounding quartz and its presence was verified with Raman spectroscopy. The coesite relic is surrounded by three omphacite crystals (omp1, omp2, omp3) with different crystallographic orientations. Scale bar = 50 µm. (**b**) Mid-IR spectra of intergranular coesite/quartz. Upper and lower spectra taken with 20 µm square apertures centered over the left and right sides of the inclusion, respectively. See text for more explanation. Spectra normalized to 1 mm thickness and shifted vertically for clarity.

Garnet shows variable replacement by amphibole along fractures. The sanidine is chemically zoned, with a thin rim increasing in Na and decreasing in K content (Sharp et al. 1992). Lastly, the amount of transformation of the coesite crystals to quartz is highly variable, from about 10 to 100%, and shows no obvious correlation with grain size or proximity to other phases (Fig. 5).

CL investigation of this sample revealed very similar features to the Dora-Maira pyrope quartzites: coesite luminesces greenish-blue, whereas quartz exhibits two CL colors—yellowish–brown for "mosaic" quartz and violet-red for palisade quartz. The infrared signatures of these phases are also virtually identical (Fig. 5). Coesite is dry within the detection limit, consistent with a previous study of these crystals (Rossman and Smyth 1990); investigation with micro-FTIR allowed us to distinguish easily between fractured and unfractured areas of the coesite crystals and confirm this result. The sharp band at 3585 cm^{-1} in quartz (chalcedony) spectra from the Dora-Maira sample is also present in all spectra taken of mosaic quartz in this sample (Fig. 5), and the range of concentrations is similar (Table 1). One difference between the samples is that analyses of palisade quartz in SRV-1 revealed measurable amounts of H_2O, in contrast to the Dora-Maira pyrope quartzite. This may reflect differing fluid-rock interaction histories for the two samples (see below).

FACTORS IN THE PRESERVATION OF COESITE

Reaction kinetics

Experimental kinetic data on the transformation of coesite to quartz were obtained by Mosenfelder and Bohlen (1997) and Perrillat et al. (2003). These studies are consistent with a kinetic model involving grain-boundary nucleation and growth of quartz from coesite, and Mosenfelder and Bohlen (1997) demonstrated that the reaction textures in their experiments were analogous to those found in natural rocks, allowing more confident extrapolation of the data. Neither set of experiments

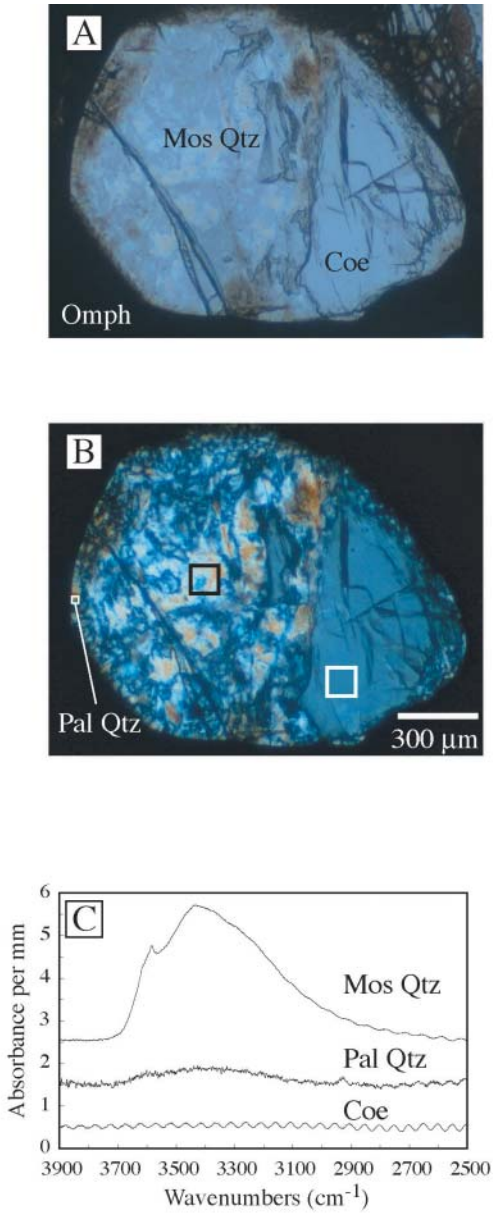

FIGURE 5. Coesite (coe) and quartz pseudomorphs in sample SRV-1 from Roberts Victor kimberlite. (**a**) Plane-polarized light. Scale bar = 300 µm. Mos Qtz = mosaic quartz; pal qtz = palisade quartz; omp = omphacite. (**b**) Cross-polarized light. Boxes show locations of analyses in c. (**c**) Mid-IR spectra. Note peak at 3585 cm^{-1} in mosaic quartz and similarity to spectrum of mosaic quartz in Figure 2b. The spectrum for coesite shows interference fringes (sinusoidal wave) resulting from reflection of the IR light off the polished surfaces of the crystal. No absorption above the level of the detection limit is detected for coesite.

provides useful constraints on nucleation rates, as the reaction was dominated by growth rates in both cases. Based on in situ X-ray diffraction (XRD) measurements, Perrillat et al. (2003) inferred higher growth rates than those measured in the quench experiments of Mosenfelder and Bohlen (1997), and a lower activation energy for growth. This disparity was conjectured by Perrillat et al. (2003) to result from the accumulation of defects in their fine-grained samples during *P-T* cycling. Another factor that may be even more important is the catalytic effect of water on growth kinetics. The use of highly hygroscopic NaCl as a pressure marker (intimately mixed with the sample in three out of five experiments) and the use of a volatile-rich pressure medium may have introduced significant amounts of water into the samples of Perrillat et al. (2003), as seen in other experimental studies of phase transformations (Kubo et al. 1998; Mosenfelder et al. 2001). The experiments of Mosenfelder and Bohlen (1997) also contained water, as the starting material was silica glass containing 425 ppm H_2O; those experiments may have gained or lost water. Unfortunately neither study provides good constraints on the progressive evolution of fluid activity in the samples with time in the experiments. Another factor that could be relevant is the development of transformation stress and strain, which can either inhibit or promote kinetics (Mosenfelder and Bohlen 1997; Mosenfelder et al. 2000).

Clearly more work is needed to explore these effects and resolve the discrepancies in available data. Nevertheless, extrapolation of the experimental data provides constraints on the survivability of coesite that are useful in assessing the importance of other factors. The extrapolation of growth rates reported by Mosenfelder and Bohlen (1997) indicates that 100 µm coesite crystals should be consumed completely at temperatures greater than about 375 °C for timescales on the order of 1 m.y. or less. Extrapolation of the data of Perrillat et al. (2003) lowers this critical temperature by about 150 °C. Such low critical temperatures confirm that other factors must be essential for the survival of coesite.

Pressure vessel hypothesis

It is now widely accepted that one of the most important factors in the preservation of coesite is its inclusion in strong, rigid minerals that act as pressure vessels, exerting an overpressure on the inclusion during exhumation. Indeed, this mechanism has recently been spectacularly demonstrated with Raman spectroscopy and synchrotron XRD data indicating present-day internal pressures on coesite crystals in garnet, zircon, and diamond as high as 3.6 GPa (Parkinson and Katayama 1999; Sobolev et al. 2000).

Similar elastic models to explain this phenomenon were developed by Gillet et al. (1984) and van der Molen and van Roermund (1986), based on the classic "sphere in a hole" problem. According to these models, small increments of reaction, allowed by kinetics and the thermoelastic response of the phases to changes in *P* and *T* during decompression, buffer the pressure on the coesite inclusion back to the equilibrium value. This process continues until the tensile strength of the host phase is exceeded and it fractures, releasing the pressure. The criterion for fracturing used by van der Molen and van Roermund (1986) is that the inclusion pressure exceeds three times the external pressure, but the actual conditions depend on the tensile strength of the host phase, which is a poorly known quantity. Nishiyama (1998) offered an improved model that considered the system as a three-shelled composite sphere (not just garnet and coesite but also quartz) and took kinetics into account; according to his

model, the pressure on the inclusion does not necessarily follow the quartz-coesite equilibrium boundary. Perrillat et al. (2003) also considered the effect of kinetics in their elastic model. An important consequence of these models is that fracturing of the host phase (using the criterion of van der Molen and van Roermund) occurs at higher temperatures for retrograde paths with a high dP/dT slope, and is also (in the latter two models) dependent on the kinetics of the transformation (for faster transformation, fracturing occurs at higher temperatures).

All of these models have been specifically developed for coesite inclusions in pyrope, which has very high elastic (bulk and shear) moduli. The models should work even better for zircon, which is stiffer than pyrope (Bass 1995). One problem with the pressure-vessel hypothesis that is rarely addressed in the literature concerns the inclusion of coesite in minerals that are much more compressible than pyrope and zircon. For such minerals, it may be difficult to sustain an internal pressure on the inclusion. For instance, dolomite has a bulk modulus (K_s) of 94.9 GPa and shear modulus (G) of 45.7 GPa (Bass 1995). These values are much lower than those of pyrope (K_s = 173 GPa, G = 92 GPa; Conrad et al. 1999) and are actually *lower* than those of coesite (K_0 = 100.8 GPa, G = 61.6 GPa; Angel et al. 2001). Other suspect hosts for coesite with relatively soft elastic moduli include tourmaline (K_0 = 100.8 GPa; Bass 1995), zoisite (K = 118–136 GPa; see Winkler et al. 2001), apatite (K_0 = 93–98 GPa, depending on OH-F substitution; Brunet et al. 1999), and wagnerite (K = 90 GPa; C. Chopin, pers. comm.). It is difficult if not impossible to reconcile these values with the pressure vessel hypothesis. Ironically, a "soft" phase such as dolomite might be an excellent "container" for coesite for the very reason that it *does not* fracture during decompression [see Figs. 1 and 2 in Schertl and Okay (1994)], thereby preventing infiltration of fluids to flux the transformation.

In addition to elasticity, the visco-elastic deformation behavior of the host phases needs to be considered. Unfortunately, flow laws for most of these phases are lacking. Dolomite single crystals can be deformed even at room temperature on laboratory timescales (e.g., Barber and Wenk 2001). Hacker and Peacock (1995) have also noted the possibility that clinopyroxene may deform by mechanical twinning at low stresses and modest temperatures, although extrapolation of the experimental mechanical data to lower strain rates is highly uncertain; moreover, this deformation mechanism has not to our knowledge been recognized in omphacite crystals containing coesite inclusions.

Finally, we note some other petrographic constraints that provide exception to the pressure-vessel hypothesis or require its modification. The process outlined here obviously cannot explain the preservation of intergranular coesite, which at present has only been found from one locality in an UHP terrane. A further complication is raised by the fact that highly variable states of preservation of coesite can sometimes be found within a single rock, thin section, or even within a single host-phase crystal (e.g., Brunet et al. 1998; Parkinson 2000; Wain et al. 2000). This may be related to different boundary constraints (the ratio of host to inclusion radii) for different inclusions, unconsidered effects of elastic anisotropy, or differences in availability of fluids. Perhaps the most spectacular example of this phenomenon comes from whiteschist garnets of the Kokchetav massif, which preserve four distinct types of silica inclusions (apparently trapped at different pressures) within a single grain of garnet: monomineralic quartz showing no evidence of reaction to or from coesite; polycrystalline quartz pseudomorphs after coesite, containing minute inclusions of hydrous minerals; well-preserved coesite crystals with palisade-quartz rims; and nearly monomineralic coesite showing no optical evidence of transformation to quartz. As shown by Parkinson (2000), this range of very different textures within a single grain attests to the importance of fluid availability in addition to the pressure-vessel effect in preserving coesite.

Exhumation rate

The use of ion-microprobe U-Pb dating of zircons and other innovative geochronological techniques has provided strong evidence that rapid exhumation is a common, if not ubiquitous, feature of UHP metamorphic rocks. Initial exhumation rates from UHP conditions of 1–3 cm/yr have been constrained for coesite-bearing rocks in the Dora-Maira massif (Gebauer et al. 1997; Rubattto and Hermann 2001), the Zermatt-Sass (Amato et al. 1999), the Western Gneiss Region of Norway (Carswell et al. 2003), the Kokchetav massif (Hermann et al. 2001; Hacker et al. 2003), and the Himalayas (Treloar et al. 2003). Clear evidence for such ultra-rapid exhumation is not yet available for the Dabie-Sulu orogen where, despite extensive geochronological investigation, the exhumation rate is "only crudely constrained to ~3–15 mm/yr" (Hacker et al. 2004, p. 166).

Following an initial period of rapid exhumation from UHP conditions to the middle or upper crust, average exhumation rates for UHP terranes slow down significantly, by up to an order of magnitude. The *P-T* conditions at which this change in exhumation rate occurs apparently vary substantially for different terranes; for instance, Gebauer et al. (1997) constrained cooling in the Dora-Maira massif to ~300 °C in 5–6 m.y., whereas rocks in the Western Gneiss Region may have cooled to only 700 °C over the same time period (Carswell et al. 2003). The residence time of rocks at high temperatures in the middle to upper crust in the Dabie-Sulu orogen is much more uncertain (Hacker et al. 2003). Better timing resolution of the latter stages of exhumation is necessary, because kinetic constraints at present (see above) suggest that fast exhumation alone may not be enough to explain the preservation of coesite in rocks that have experienced high-temperature retrograde metamorphism at shallower levels in the crust.

P-T path

Chopin (1984), on the basis of talc + phengite stability in pyrope-quartzites, constrained a *P-T* path for the Dora-Maira UHP rocks marked by continuous cooling during decompression. Furthermore, based on their elastic model, Gillet et al. (1984) rejected the possibility of isothermal decompression because fracturing of garnet-containing coesite would occur at too high a temperature to allow preservation of coesite, according to estimates of reaction kinetics at that time. Thus, continuous cooling during decompression was thought to be a key factor in the preservation of coesite inclusions.

Subsequent to these studies, high-temperature, low-pressure metamorphic overprints were recognized in UHP rocks from Weihai (Wang et al. 1993) and Rongcheng County (Nakamura

TABLE 2. H_2O/OH concentrations in opal from Dora Maira sample 19485

d (cm)	Ai		ρ (g/cm³)	C (H_2O), wt%		
	5200 cm^{-1}	4450 cm^{-1}		$(H_2O)_{mol}$	OH	$(H_2O)_{tot}$
0.008	11.2495	3.45025	2.1	4.82	2.31	7.13
			2.6	3.89	1.87	5.76

Note: Concentrations shown for end-member values for density.

and Hirajima 2000) in the Sulu orogen in eastern China. The geographical distribution of these rocks suggests that these are not isolated blocks but that significant portions of the northeastern part of the Sulu region may have experienced these conditions (Nakamura and Hirajima 2000). Reconstructed retrograde *P-T* paths for these rocks entail isothermal or nearly isothermal decompression (Zhang et al. 1995b; Banno et al. 2000; Nakamura and Hirajima 2000) or perhaps slight heating during decompression (Wang et al. 1993; Banno et al. 2000). Isothermal decompression at high temperatures has also been documented for UHP rocks in the Variscan French Massif Central (Lardeaux et al. 2001) and in the Lanterman Range in Antarctica (Ghiribelli et al. 2002), where evidence for UHP metamorphism is more questionable. Finally, upper amphibolite-facies or granulite-facies overprints have also been inferred for the Western Gneiss Region of Norway (e.g., Carswell et al. 2003) and the Kokchetav massif (e.g., Hermann et al. 2001), although the retrograde *P-T* paths derived for these UHP rocks do involve continuous cooling (at higher temperatures than in the western Alps). Ernst (1999), offering an explanation for the preservation of coesite in these rocks, suggested that the early stages of decompression in cases where nearly isothermal decompression is inferred might actually have retraced the prograde *P-T* trajectory prior to the high-temperature overprint (cf., Harley and Carswell 1995), but there is no petrological evidence to support such a "hidden" *P-T* trajectory. Note that Ernst's elegant "thin slab" model for exhumation (e.g., Ernst 1999) is difficult to reconcile with the evidence for nearly adiabatic decompression because thin slabs (<10 km) must gain or lose heat unless exhumation is extraordinarily rapid (Nakamura and Hirajima 2000; Roselle and Engi 2002).

Based on these occurrences, continuous cooling during decompression does not appear to be necessary for the preservation of coesite. Furthermore, if the predictions from elastic models are correct, host phases for coesite should fracture at high temperatures for rocks that experience isothermal decompression; even the fastest exhumation rates documented for UHP rocks are unlikely to save coesite from complete obliteration in such cases.

Fluid infiltration

Restricted fluid flow during UHP peak metamorphism and retrogression during exhumation is an increasingly recognized phenomenon. Primary evidence comes from the partial preservation of igneous assemblages and/or textures in UHP rocks (Biino and Compagnoni 1992; Liou and Zhang 1997; Wallis et al. 1997; Chopin 2003), preservation of pre-metamorphic O-isotope anomalies (Zheng et al. 2003), and local-scale fluid inclusion studies (Philippot et al. 1995; Fu et al. 2001). The finding of intergranular coesite in an UHP terrane that may not have experienced ultra-rapid (>1 cm/m.y.) exhumation has also been used to suggest a lack of fluid availability during retrogression (Liou and Zhang 1996). Our finding of trace amounts of H_2O in quartz replacing this intergranular coesite is surprising and suggests that fluid infiltration must have occurred at very low temperatures for the coesite to survive. The variable state of preservation of the intergranular coesite (compare Fig. 4a to Liou and Zhang 1996) may reflect very localized fluid infiltration in this rock.

In the case of the Dora-Maira massif, our data support a multi-stage history for the transformation of coesite to quartz, punctuated by one or more discrete fluid infiltration events. Palisade quartz formed under relatively dry conditions early in the transformation. The sparse fluid inclusions contained in this quartz probably represent water that was trapped in coesite during its formation by the reaction: talc + kyanite = pyrope + coesite + H_2O (Chopin 1984) and then partitioned into quartz during the transformation. Note that this water was most likely in the form of fluid inclusions, not structurally bound hydroxyl (cf., Langenhorst and Poirier 2002), because the solubility of OH in coesite at the peak conditions of metamorphism is very low (Mosenfelder 2000). Another source of these early fluids could have been fluid inclusions in pyrope, inferred from the presence of "negative crystals" now containing fine-grained secondary phyllosilicates (see Fig. 3d in Schertl et al. 1991). During decompression, water activity progressively increased as a result of crystallization of and expulsion of water-rich fluids from partial melt (Sharp et al. 1993; Philippot et al. 1995). However, the coesite crystals must have been buffered from this fluid activity by the un-fractured host phase. The formation of the diffuse quartz (or chalcedony) and microcrystalline opal—only micrometers away from unreacted coesite crystals—must have occurred at very low temperatures because of the high water contents of these phases. Formation temperatures of chalcedony are typically estimated to be less than 250 °C (Graetsch et al. 1985). Moreover, kinetic constraints prohibit partial preservation of coesite under such hydrous conditions if temperatures are high.

The remarkable similarity of transformation textures and fluid signatures in the Roberts Victor sample (SRV-1) to those of the Dora-Maira pyrope quartzites paints a similar picture of the history of the transformation, albeit contracted over a much shorter time period (on the order of hours or days instead of millions of years). In the case of SRV-1, fluids may have been locally derived from the breakdown of other phases in the rock. Vacancy rich omphacite, the most abundant phase in SRV-1, is known to incorporate large amounts of OH (Smyth et al. 1991). H_2O may also have come from the breakdown of K-cymrite, a high-pressure hydrous phase, to sanidine. Although there is no direct evidence for such a transformation, FTIR measurements have shown that the sanidine in this rock contains fluid inclusions (Rossman and Smyth 1990). Based on the lack of melting in the sample, the preservation of high-temperature disorder in sanidine and the preservation of ultra high-temperature O-isotope fractionations, Sharp et al. (1992) inferred that rapid decompression took place under anhydrous conditions. The evolution of the large amounts of H_2O necessary to produce chalcedony after coesite therefore probably took place during the later stages of the xenolith's ascent to the surface.

Our survey of coesite and its pseudomorphs in UHP rocks is far from comprehensive, and the most conclusive results come from two unusual samples. Nevertheless, the results are consis-

tent with lack of fluid availability being a critical factor in the preservation of coesite. The best-preserved inclusions, such as the one shown in Figure 3a, probably survive not only because of their incorporation in a strong host phase but because of the ability of the host to prevent fluid infiltration until fracturing occurs at low temperatures.

ACKNOWLEDGMENTS

We are honored to present this paper in tribute to Gary Ernst and are grateful for his inspiration and encouragement on this project. This paper is also dedicated in memoriam to Alice Wain, who donated the Norwegian eclogite samples. We thank Hubert Schulze (Bayreuth) and the Bochum preparation team for expert thin section preparation. Thanks also go to Rolf Neuser, who made the CL-investigations possible. Christian Chopin, Bradley Hacker, and Ikuo Katayama provided valuable, constructive reviews. Thanks also to George Rossman and Christian Chopin for helpful discussions. J.L.M. thanks the Bayerisches Geoinstitut, Bayreuth, for financial support in the early stages of this seemingly never-ending project.

REFERENCES CITED

Aines, R.D., Kirby, S.H., and Rossman, G.R. (1984) Hydrogen speciation in synthetic quartz. Physics and Chemistry of Minerals, 11, 204–212.

Amato, J.M., Johnson, C.M., Baumgartner, L.P., and Beard, B.L. (1999) Rapid exhumation of the Zermatt-Sass ophiolite deduced from high-precision Sm-Nd and Rb-Sr geochronology. Earth and Planetary Science Letters, 171, 425–438.

Angel, R.J., Mosenfelder, J.L., and Shaw, C.S.J. (2001) Anomalous compression and equation of state of coesite. Physics of the Earth and Planetary Interiors, 124, 71–79.

Banno, S., Enami, M., Hirajima, T., Ishiwatari, A., and Wang, Q.C. (2000) Decompression P-T path of coesite eclogite to granulite from Weihai, eastern China. Lithos, 52, 97–108.

Barber, D.J. and Wenk, H.-R. (2001) Slip and dislocation behaviour in dolomite. European Journal of Mineralogy, 13, 221–243.

Bass, J. (1995) Elasticity of minerals, glasses, and melts. In T.J. Ahrens, Ed., Mineral physics and crystallography: a handbook of physical constants, 2, p. 45–63. American Geophysical Union, Washington, D.C.

Biino, G. and Compagnoni, R. (1992) Very high pressure metamorphism of the Brosassco coronite metagranite, southern Dora-Maira massif, western Alps. Schweizerische Mineralogische und Petrographische Mitteilungen, 72, 347–363.

Boyer, H., Smith, D.C., Chopin, C., and Lasnier, B. (1985) Raman microprobe (RMP) determinations of natural and synthetic coesite. Physics and Chemistry of Minerals, 12, 45–48.

Brunet, F., Chopin, C., and Seifert, F. (1998) Phase relations in the MgO-P_2O_5-H_2O system and the stability of phosphoellenbergerite: petrological implications. Contributions to Mineralogy and Petrology, 131, 54–70.

Brunet, F., Allan, D.R., Redfern, S.A.T., Angel, R.J., Miletich, R., Reichmann, H.J., Sergent, J., and Hanfland, M. (1999) Compressibility and thermal expansivity of synthetic apatites, $Ca_5(PO_4)_3X$ with X = OH, F and CL. European Journal of Mineralogy, 11, 1023–1035.

Carswell, D.A., Brueckner, H.K., Cuthbert, S.J., Mehta, K., and O'Brien, P.J. (2003) The timing of stabilisation and the exhumation rate for ultra-high pressure rocks in the Western Gneiss Region of Norway. Journal of Metamorphic Geology, 21, 601–612.

Chopin, C. (1984) Coesite and pure pyrope in high-grade blueschists of the Western Alps: a first record and some consequences. Contributions to Mineralogy and Petrology, 86, 107–118.

———(2003) Ultrahigh-pressure metamorphism: tracing continental crust into the mantle. Earth and Planetary Science Letters, 212, 1–14.

Conrad, P.G., Zha, C.-S., Mao, H.-K., and Hemley, R.J. (1999) The high-pressure, single crystal elasticity of pyrope, grossular, and andradite. American Mineralogist, 84, 374–383.

Cuthbert, S.J., Carswell, D.A., Krogh-Ravna, E.J., and Wain, A. (2000) Eclogites and eclogites in the Western Gneiss Region, Norwegian Caledonides. Lithos, 52, 165–195.

Enami, M., Liou, J.G., and Mattinson, C.G. (2004) Epidote minerals in high P/T metamorphic terranes: subduction zone and high- to ultrahigh-pressure metamorphism. In A. Liebscher and G. Franz, Eds. Epidotes, Reviews in Mineralogy 56, p. 347–398. Mineralogical Society of America, Washington, D.C.

Ernst, W.G. (1999) Metamorphism, partial preservation, and exhumation of ultrahigh-pressure belts. The Island Arc, 8, 125–153.

———(2001) Subduction, ultrahigh-pressure metamorphism, and regurgitation of buoyant crustal slices—implications for arcs and continental growth. Physics of the Earth and Planetary Interiors, 127, 253–275.

Fu, B., Touret, J.L.R., and Zheng, Y.-F. (2001) Fluid inclusions in coesite-bearing eclogites and jadeite quartzite at Shuanghe, Dabie Shan (China). Journal of Metamorphic Geology, 19, 531–547.

Gebauer, D., Schertl, H.-P., Brix, M., and Schreyer, W. (1997) 35 Ma old ultrahigh-pressure metamorphism and evidence for very rapid exhumation in the Dora Maira massif, Western Alps. Lithos, 41, 5–24.

Ghiribelli, B., Frezzotti, M.-L., and Palmeri, R. (2002) Coesite in eclogites of the Lanterman Range (Antarctica): evidence from textural and Raman studies. European Journal of Mineralogy, 14, 355–360.

Gillet, P., Ingrin, J., and Chopin, C. (1984) Coesite in subducted continental crust: P-T history deduced from an elastic model. Earth and Planetary Science Letters, 70, 426–436.

Graetsch, H. (1994) Structural characteristics of opaline and microcrystalline silica minerals. In P.T. Heaney, C.T. Prewitt, and G.V. Gibbs, Eds., Silica: physical behavior, geochemistry and materials applications, 29, p. 209–232. Reviews in Mineralogy, Mineralogical Society of America, Washington, D.C.

Graetsch, H., Floerke, O.W., and Miehe, G. (1985) The nature of water in chalcedony and opal-C from Brazilian agate nodes. Physics and Chemistry of Minerals, 12, 300–306.

Hacker, B.R. and Peacock, S.M. (1995) Creation, preservation and exhumation of UHPM rocks. In R.G. Coleman, and X. Wang, Eds., Ultrahigh Pressure Metamorphism, p. 159–181. Cambridge University Press. Cambridge, U.K.

Hacker, B.R., Calvert, A., Zhang, R.Y., Ernst, W.G., and Liou, J.G. (2003) Ultrarapid exhumation of ultrahigh-pressure diamond-bearing metasedimentary rocks of the Kokchetav Massif, Kazakhstan? Lithos, 70, 61–75.

Hacker, B.R., Ratschbacher, L. and Liou, J.G. (2004) Subduction, collision and exhumation in the ultrahigh-pressure Qinling-Dabie orogen: A review. In J. Malpas, C.J.N. Fletcher, J.R. Ali, and J.C. Aitchison, Eds., Aspects of the Tectonic Evolution of China. Special Paper 226, Geological Society of London, p. 157–175.

Harley, S.L. and Carswell, D.A. (1995) Ultradeep crustal metamorphism: a prospective view. Journal of Geophysical Research, 100, 8367–8380.

Hermann, J., Rubatto, D., Korsakov, A., and Shatsky, V.S. (2001) Multiple zircon growth during fast exhumation of diamondiferous, deeply subducted continental crust (Kokchetav Massif, Kazakhstan). Contributions to Mineralogy and Petrology, 141, 66–82.

Ingrin, J. and Gillet, P. (1986) TEM investigation of the crystal microstructures in a quartz-coesite assemblage of the western Alps. Physics and Chemistry of Minerals, 13, 325–330.

Kronenberg, A.K. and Wolf, G.H. (1990) Fourier transform infrared spectroscopy determinations of intragranular water content in quartz-bearing rocks: implications for hydrolytic weakening in the laboratory and within the Earth. Tectonophysics, 172, 255–271.

Kubo, T., Ohtani, E., Kato, T., Shinmei, T., and Fujino, K. (1998) Experimental investigation of the α–β transformation of San Carlos olivine single crystal. Physics and Chemistry of Minerals, 26, 1–6.

Langenhorst, F. and Poirier, J.-P. (2002) Transmission electron microscopy of coesite inclusions in the Dora Maira high-pressure metamorphic pyrope-quartzite. Earth and Planetary Science Letters, 203, 793–803.

Langer, K. and Flörke, O.W. (1974) Near infrared absorption spectra (4000–9000 cm^{-1}) of opals and the role of "water" in these SiO_2-nH_2O minerals. Fortschritte der Mineralogie, 52, 17–51.

Lardeaux, J.-M., Ledru, P., Daniel, I., and Duchene, S. (2001) The Variscan French Massif Central—a new addition to the ultra-high pressure metamorphic 'club': exhumation processes and geodynamic consequences. Tectonophysics, 332, 143–167.

Libowitzky, E. and Rossman, G.R. (1997) An IR absorption calibration for water in minerals. American Mineralogist, 82, 1111–1115.

Liou, J.G. and Zhang, R.Y. (1996) Occurrences of intergranular coesite in ultrahigh-P rocks from the Sulu region, eastern China: implications for lack of fluid during exhumation. American Mineralogist, 81, 1217–1221.

Liou, J.G., Zhang, R.Y., and Jahn, B.-M. (1997) Petrology, geochemistry and isotope data on a ultrahigh-pressure jadeite quartzite from Shuanghe, Dabie Mountains, East-central China. Lithos, 41, 59–78.

Mosenfelder, J.L. (2000) Pressure dependence of hydroxyl solubility in coesite. Physics and Chemistry of Minerals, 27, 610–617.

Mosenfelder, J.L. and Bohlen, S.R. (1997) Kinetics of the coesite to quartz transformation. Earth and Planetary Science Letters, 153, 133–147.

Mosenfelder, J.L., Connolly, J.A.D., Rubie, D.C., and Liu, M. (2000) Strength of $(Mg,Fe)_2SiO_4$ wadsleyite determined by relaxation of transformation stress. Physics of the Earth and Planetary Interiors, 120, 63–78.

Mosenfelder, J.L., Marton, F.C., Ross II, C.R., Kerschhofer, L., and Rubie, D.C. (2001) Experimental constraints on the depth of olivine metastability in subducting lithosphere. Physics of the Earth and Planetary Interiors, 127, 165–180.

Nakamura, D. and Hirajima, T. (2000) Granulite-facies overprinting of ultrahigh-pressure metamorphic rocks, Northeastern Su-Lu region, Eastern China. Journal of Petrology, 41, 563–582.

Nakashima, S., Matayoshi, H., Yuko, T., Michibayashi, K., Masuda, T., Kuroki, N., Yamagishi, H., Ito, Y., and Nakamura, A. (1995) Infrared microspectroscopy analysis of water distribution in deformed and metamorphosed rocks.

Tectonophysics, 245, 263–276.
Nishiyama, T. (1998) Kinetic modeling of the coesite-quartz transition in an elastic field and its implication for the exhumation of ultrahigh-pressure metamorphic rocks. The Island Arc, 7, 70–81.
Ostrooumov, M., Fritsch, E., Lasnier, B., and Lefrant, S. (1999) Spectres Raman des opales: aspect diagnostique et aide a la classification. European Journal of Mineralogy, 11, 899–908.
Parkinson, C.D. (2000) Coesite inclusions and prograde compositional zonation of garnet in whiteschist of the HP-UHPM Kokchetav massif, Kazakhstan: a record of progressive UHP metamorphism. Lithos, 52, 215–233.
Parkinson, C.D. and Katayama, I. (1999) Present-day ultrahigh-pressure conditions of coesite inclusions in zircon and garnet: evidence from laser Raman microspectroscopy. Geology, 27, 979–982.
Perrillat, J.P., Daniel, I., Lardeaux, J.M., and Cardon, H. (2003) Kinetics of the coesite-quartz transition: application to the exhumation of ultrahigh-pressure rocks. Journal of Petrology, 44, 773–788.
Philippot, P., Chevallier, P., Chopin, C., and Dubessy, J. (1995) Fluid composition and evolution in coesite-bearing rocks (Dora-Maira massif, Western Alps): implications for element recycling during subduction. Contributions to Mineralogy and Petrology, 121, 29–44.
Reinecke, T. (1991) Very-high-pressure metamorphism and uplift of coesite-bearing metasediments from the Zermatt-Sass zone, Western Alps. European Journal of Mineralogy, 3, 7–17.
——— (1998) Prograde high- to ultrahigh-pressure metamorphism and exhumation of oceanic sediments at Lago di Cignana, Zermatt-Saas zone, western Alps. Lithos, 42, 147–189.
Roselle, G.T. and Engi, M. (2002) Ultra high pressure (UHP) terrains: lessons from thermal modeling. American Journal of Science, 302, 410–441.
Rossman, G.R. and Smyth, J.R. (1990) Hydroxyl contents of accessory minerals in mantle eclogites and related rocks. American Mineralogist, 75, 775–780.
Rubatto, D. and Hermann, J. (2001) Exhumation as fast as subduction? Geology, 29, 3–6.
Schertl, H.-P. and Okay, A.I. (1994) A coesite inclusion in dolomite in Dabie Shan, China: petrological and rheological significance. European Journal of Mineralogy, 6, 995–1000.
Schertl, H.-P., Schreyer, W., and Chopin, C. (1991) The pyrope-coesite rocks and their country rocks at Parigi, Dora Maira Massif, Western Alps: detailed petrography, mineral chemistry and P-T path. Contributions to Mineralogy and Petrology, 108, 1–21.
Schertl, H.-P., Neuser, R.D., Sobolev, N.V., and Shatsky, V.S. (2004) UHP-metamorphic rocks from Dora Maira/Western Alps and Kokchetav/Kazakhstan: new insights using cathodoluminescence petrography. European Journal of Mineralogy, 16, 49–57.
Sharp, Z.D., Essene, E.J., and Smyth, J.R. (1992) Ultra-high temperatures from oxygen isotope thermometry of a coesite-sanidine grospydite. Contributions to Mineralogy and Petrology, 112, 358–370.
Sharp, Z.D., Essene, E.J., and Hunziker, J.C. (1993) Stable isotope geochemistry and phase equilibria of coesite-bearing whiteschists, Dora Maira Massif, western Alps. Contributions to Mineralogy and Petrology, 114, 1–12.
Smith, D.C. (1984) Coesite in clinopyroxene in the Caledonides and its implications for geodynamics. Nature, 310, 641–644.
Smyth, J.R. (1977) Quartz pseudomorphs after coesite. American Mineralogist, 62, 828–830.
——— (1980) Cation vacancies and the crystal chemistry of breakdown reactions in kimberlitic omphacites. American Mineralogist, 65(1185–1191).
Smyth, J.R. and Hatton, C.J. (1977) A coesite-sanidine grospydite from the Roberts Victor kimberlite. Earth and Planetary Science Letters, 77, 284–290.
Smyth, J.R., Bell, D.R., and Rossman, G.R. (1991) Incorporation of hydroxyl in upper-mantle clinopyroxenes. Nature, 351, 732–735.
Sobolev, N.V., Yefimova, E.S., Koptil, V.I., Lavrent'ev, Y.G., and Sobolev, V.S. (1976) Coesite, garnet and omphacite inclusions in Yakut diamonds—first finding of coesite paragenesis. Doklady Akademii Nauk, SSSR, 230, 1442–1444. (In Russian.)
Sobolev, N.V., Fursenko, B.A., Goryainov, S.V., Shu, J., Hemley, R.J., Mao, H.-K., and Boyd, F.R. (2000) Fossilized high pressure from the Earth's deep interior: the coesite-in-diamond barometer. Proceedings of the National Academy of Sciences, 97, 11875–11879.
Thomsen, V., Schatzlein, D., and Mercuro, D. (2003) Limits of detection in spectroscopy. Spectroscopy, 18 (12), 112–114.
Treloar, P.J., O'Brien, P.J., Parrish, R.R., and Khan, M.A. (2003) Exhumation of early Tertiary, coesite-bearing eclogites from the Pakistan Himalaya. Journal of the Geological Society, London, 160, 367–376.
Van der Molen, I. and Van Roermund, H.L.M. (1986) The pressure path of solid inclusions in minerals: The retention of coesite inclusions during uplift. Lithos, 19, 317–324.
Wain, A. (1997) New evidence for coesite in eclogite and gneisses - defining an ultrahigh-pressure province in the Western Gneiss Region of Norway. Geology, 25, 927–930.
Wain, A., Waters, D., Jephcoat, A., and Olijynk, H. (2000) The high-pressure to ultrahigh-pressure eclogite transition in the Western Gneiss Region, Norway. European Journal of Mineralogy, 12, 667–687.
Wallis, S.R., Ishiwatari, A., Hirajima, T., Ye, K., Guo, J., Nakamura, D., Kato, T., Zhai, M., Enami, M., Cong, B., and Banno, S. (1997) Occurrence and field relationships of ultrahigh-pressure metagranitoid and coesite eclogite in the Su-Lu terrane, eastern China. Journal of the Geological Society, London, 154, 45–54.
Walsh, E.O. and Hacker, B.R. (2004) The fate of subducted continental margins: two-stage exhumation of the high-pressure to ultrahigh-pressure Western Gneiss Region, Norway. Journal of Metamorphic Geology, 22, 671–687.
Wang, Q., Ishiwatari, A., Zhao, Z., Hirajima, T., Hiramitsu, N., Enami, M., Zhai, M., Li, J., and Cong, B. (1993) Coesite-bearing granulite retrograded from eclogite in Weihai, eastern China. European Journal of Mineralogy, 5, 141–152.
Winkler, B., Milman, V., and Nobes, R.H. (2001) A theoretical investigation of the relative stabilities of Fe-free clinozoisite and orthozoisite. Physics and Chemistry of Minerals, 28, 471–474.
Wohletz, K.H. and J.R. Smyth (1984) Origin of a sanidine-coesite grospydite: thermodynamic considerations. In J. Kornprobst, Ed., Kimberlites II: The Mantle and Crust-Mantle Relationships, p. 33–42. Elsevier, Amsterdam (Netherlands).
Xu, H., Buseck, P.R., and Luo, G. (1998) HRTEM investigation of microstructures in length-slow chalcedony. American Mineralogist, 83, 542–545.
Zhang, R.Y. and Liou, J.G. (1996) Coesite inclusions in dolomite from eclogite in the southern Dabie Mountains, China: the significance of carbonate minerals in UHPM rocks. American Mineralogist, 81, 181–186.
——— (1997) Partial transformation of gabbro to coesite-bearing eclogite from Yangkou, the Sulu Terrane, eastern China. Journal of Metamorphic Geology, 15, 183–202.
Zhang, R.Y., Liou, J.G., and Cong, B.L. (1995a) Talc-, magnesite- and Ti-clinohumite- bearing ultrashigh-pressure meta-mafic and ultramafic complex in the Dabie Mountains, China. Journal of Petrology, 36, 1011–1037.
Zhang, R.Y., Liou, J.G., and Ernst, W.G. (1995b) Ultrahigh-pressure metamorphism and decompressional P-T paths of eclogites and country rocks from Weihai, eastern China. The Island Arc, 4, 293–309.
Zheng, Y.-F., Fu, B., Gong, B., and Li, L. (2003) Stable isotope geochemistry of ultrahigh pressure metamorphic rocks from the Dabie-Sulu orogen in China: implications for geodynamics and fluid regime. Earth-Science Reviews, 62, 105–161.

MANUSCRIPT RECEIVED APRIL 27, 2004
MANUSCRIPT ACCEPTED JANUARY 19, 2005
MANUSCRIPT HANDLED BY WILLIAM CARLSON